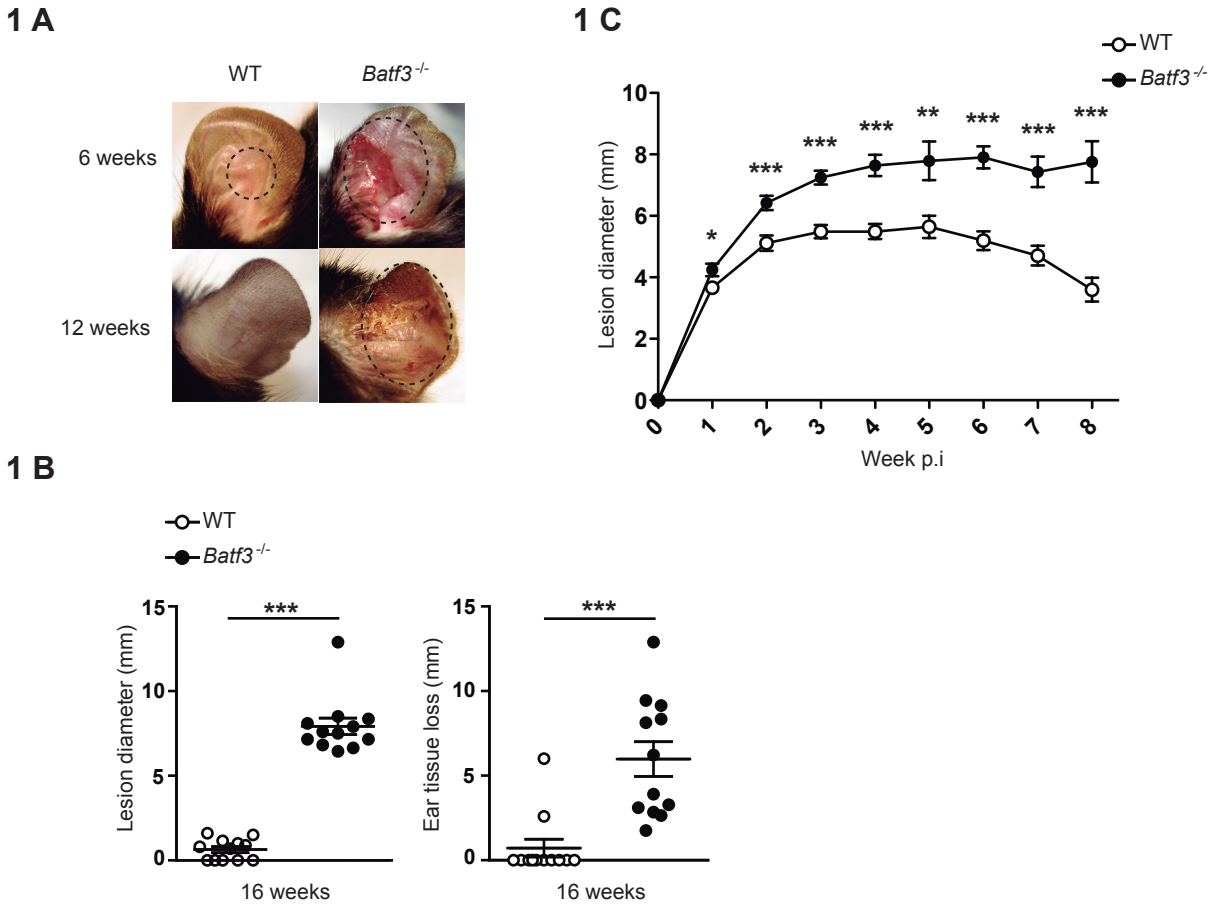

Supporting information Figure 1. Batf3-deficient mice develop exacerbated and unresolved pathology following *L. major* infection. (A) Representative images of ear pinnae of WT and Batf3$^{-/-}$ mice 6 and 12 weeks after infection in the ear pinnae with 1000 *L. major* parasites. (B) Lesion diameter (left) and ear tissue loss (right) was quantified in WT and Batf3-deficient mice 16 weeks p.i. Individual data and arithmetic mean ± SEM from one representative experiment of three performed are shown. (C) Progression of lesion diameter in WT and Batf3$^{-/-}$ mice infected i.d. in the ear pinnae with 5x10^4 *L. major* parasites. Data are arithmetic mean ± SEM (n=22) from one representative experiment of three performed.

2 A

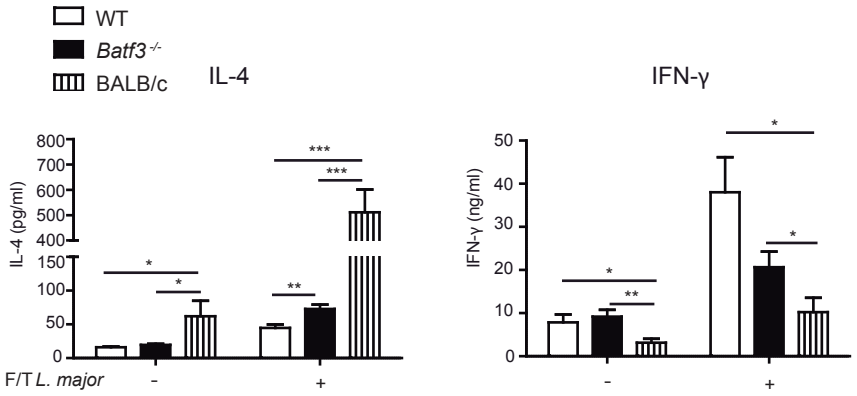

2 B

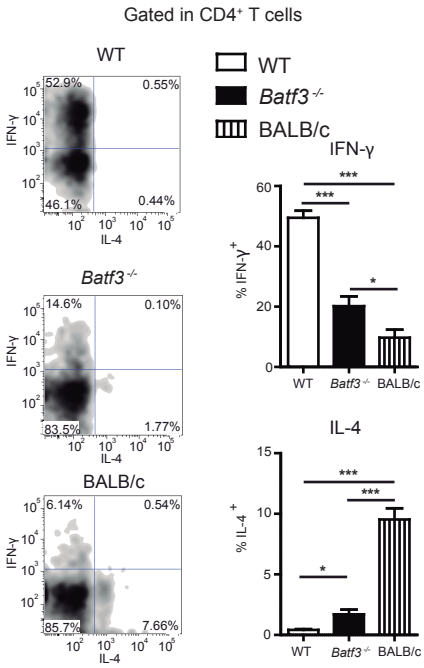

2 C

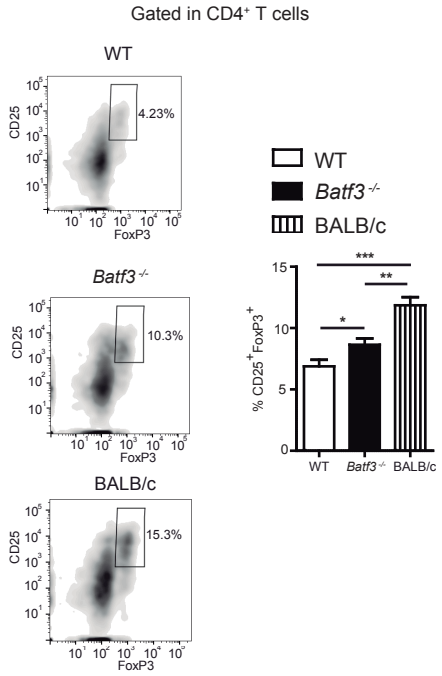

Supporting information Figure 2. Skewed immunity in Batf3$^{-/-}$ mice is milder compared with Balb/c mice. WT and Batf3$^{-/-}$ C57BL/6 and Balb/c mice were infected i.d. with 5x10^4 *L. major* parasites. (A) Draining LN cells obtained 3 weeks p.i. (2 x 10^6) were restimulated with freeze-thawed (F/T) *L. major*, and IL-4 and IFN-γ were measured in the supernatant. Histograms show arithmetic mean + SEM of a representative experiment (n=5) of three performed. (B, C) Ear cell suspensions were restimulated with anti-CD3 and anti-CD28 to measure IFN-γ (B) or analysed for FoxP3 levels in steady state (C). Representative plots and graphs with arithmetic mean + SEM of a representative experiment (n=5) of three performed.

3 A

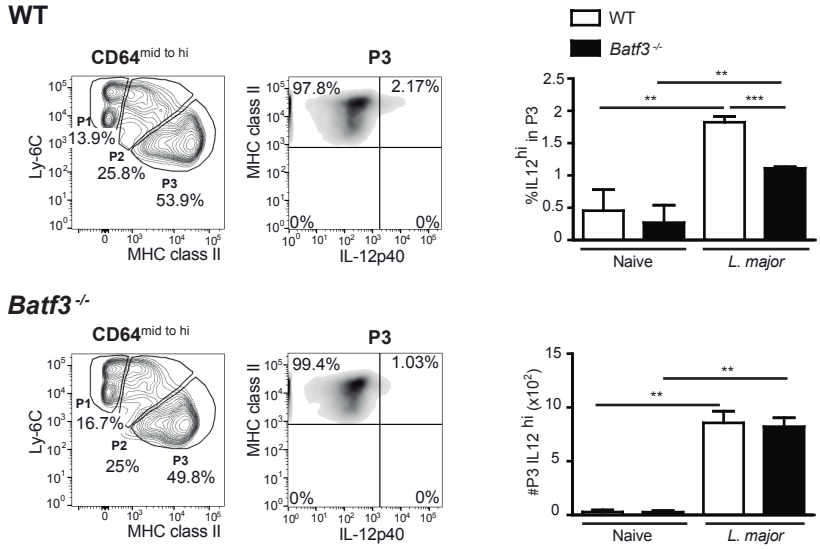

3 B

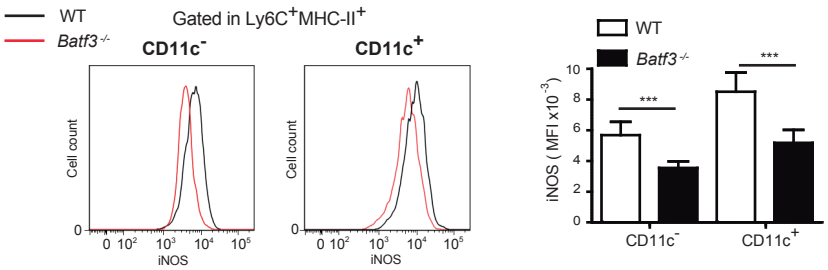

Supporting information Figure 3. Batf3 deficiency partially affects monocyte-derived DC and macrophage function. WT and Batf3$^{-/-}$ mice infected with 5 x 10^4 *L. major* parasites were injected with Brefeldin A (250 µg i.p.) 2 weeks p.i. and analysed 5h later. (A) dLN cells were stained for Ly6C, CD64, MHC class II, and intracellular IL-12p40. Left: staining of P1, P2 and P3 populations; Right: graphs showing average frequency and absolute numbers of P3 moDCs expressing high levels of IL-12p40 (n= 5). (B) Macrophages (Ly6C$^+$CD11c$^-$MHC-II$^+$) and monocyte-derived DCs (Ly6C$^+$CD11c$^+$MHC-II$^+$) were further analysed for iNOS expression by flow cytometry at 3 weeks p.i. (n=10). (A, B) Representative plots and graphs with arithmetic mean + SEM of a representative experiment of three performed.

4 A

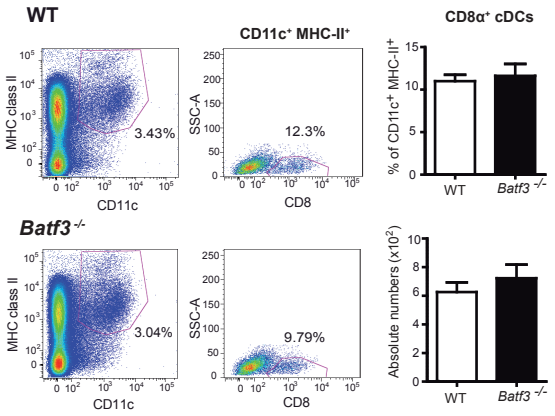

4 B

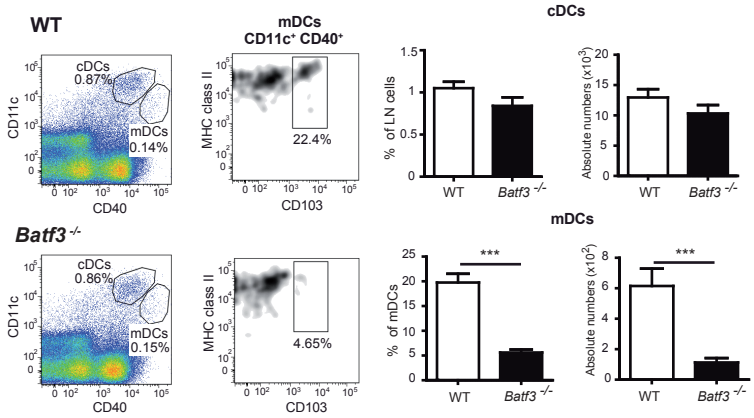

4 C

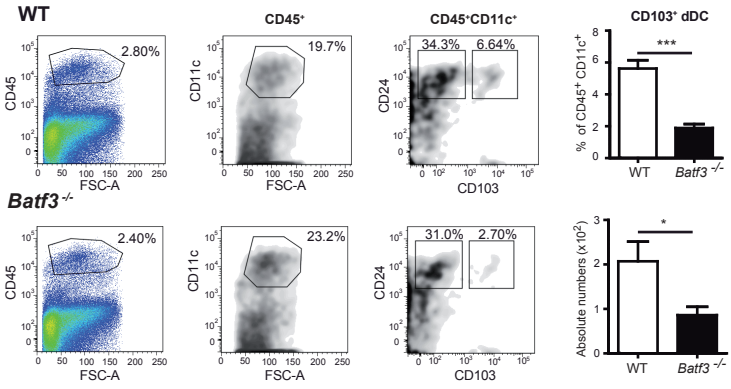

Supporting information Figure 4. Analysis of Batf3-dependent DCs in skin-draining LN and skin. (A) Skin draining LNs from WT and Batf3$^{-/-}$ mice were analysed for CD11c, MHC class II and CD8. Left: one representative plot series shown for gating. Right: frequency (upper panel) and absolute numbers (lower panel) of CD8α^{+} DCs. (B) Skin draining LN from WT and Batf3$^{-/-}$ mice were analysed for CD11c, CD40, MHC class II and CD103. Left: one representative plot series shown for gating. Right: Frequency and absolute numbers of conventional DCs (cDCs) (upper panel) and migratory DCs (mDCs) (lower panel). (C) Ears from WT and Batf3$^{-/-}$ mice were processed to cell suspensions and analysed for CD45, CD11c, CD24 and CD103. Left: one representative plot series is shown for gating strategy. Right: frequency (upper panel) and absolute numbers (lower panel) of CD103^{+} dDCs recovered per ear. (A-C) Graphs with arithmetic mean + SEM of a representative experiment (n=5) of three performed.

5 A

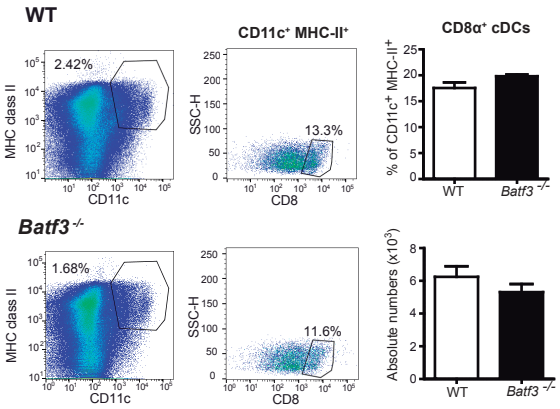

5 B

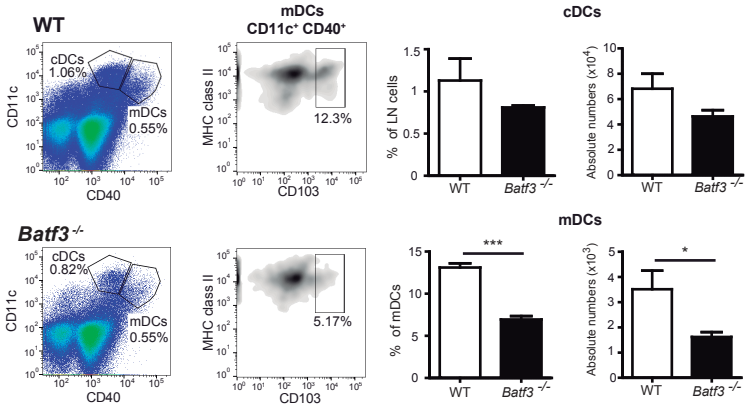

5 C

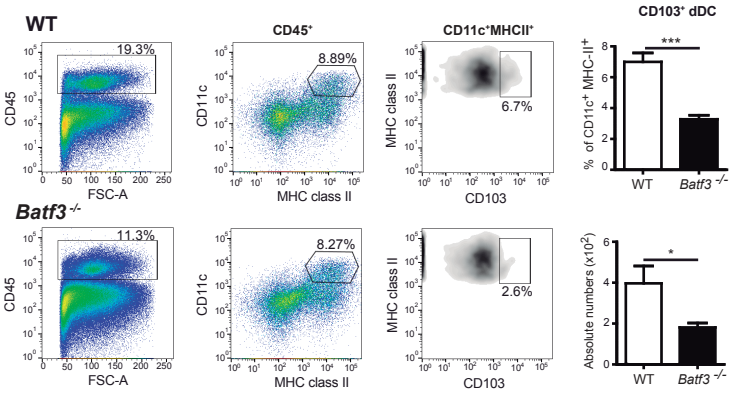

Supporting information Figure 5. Analysis of Batf3-dependent DCs in skin-draining LN and skin following *Leishmania* infection. WT and Batf3$^{-/-}$ mice were infected with 5 x 10^4 *L. major* parasites and analysed 2 weeks p.i (A) Skin draining LN from WT and Batf3$^{-/-}$ mice were analysed for CD11c, MHC class II and CD8. Left: one representative plot series shown for gating. Right: frequency (upper panel) and absolute numbers (lower panel) of CD8α$^+$ DCs. (B) Skin draining LN from WT and Batf3$^{-/-}$ mice were analysed for CD11c, CD40, MHC class II and CD103. Left: one representative plot series shown for gating. Right: Frequency and absolute numbers of conventional DCs (cDCs) (upper panel) and migratory DCs (mDCs) (lower panel). (C) Ears from WT and Batf3$^{-/-}$ mice were processed to cell suspensions and analysed for CD45, CD11c, MHC class II and CD103. Left: one representative plot series is shown for gating strategy. Right: frequency (upper panel) and absolute numbers (lower panel) of